

## An Investigation of a Zero-Net-Mass-Flux Jet in Cross Flow using PIV

C. J. Dillon-Gibbons, C.Y. Wong and J. Soria

Laboratory for Turbulent Research in Aerospace and Combustion  
Monash University, Melbourne, Victoria, 3800 AUSTRALIA

### Abstract

Zero-Net-Mass-Flux Jets in cross flow can be used in a number of engineering applications, such as combustion in a gas turbine engine and the cooling of turbine blades. ZNMF-Jets have been seen to create two distinct flow regimes when impinging into a flow, either singular or multiple trajectories as characterised by the Strouhal Number. This paper shows two cases for a ZNMF-Jet in Cross-flow, when the flow is singular and when the flow shows multiple trajectories, using Digital Particle Image Velocimetry (DPIV). Time and Phase-averaged experiments were conducted in a vertical water tunnel, where the ZNMF-Jet was created using a stepper motor scotch-yoke piston arrangement of cylinder diameter 20mm to force fluid through a 10mm circular jet orifice. The Strouhal Number was taken at 0.11 and 0.56 with the Reynolds Number held constant at 1066 and the velocity ratio between the free stream and the r.m.s. fluctuating velocities of the ZNMF - Jet also held constant at 2. The depth of penetration of the ZNMF-Jet into the cross flow decreases with an increase in Strouhal Number, while the strength of the vortical structures increases with increasing Strouhal Number.

### Introduction

The phenomena of jets in cross flow have a number of important applications in engineering including combustion engines, STOVL (Short Take Off Vertical Landing) aircraft, turbine blade cooling and missile control systems to name but a few. However the field structures of a jet in cross flow have a very turbulent nature and extensive research has been undertaken in an attempt to understand and develop a model for this flow.

A zero-net-mass-flux jet (ZNMF) is an oscillating jet where the flow from the jet is not continuous. Typically the jet is mechanically forced in a sinusoidal nature where the jet has two stages, exhaust and intake of fluid. The important aspect of the zero-net-mass-flux jet is that it does not impart mass into the system instead it acts to add momentum to the system through the interaction of vortices. The vortices are produced during the exhaust stroke of the jet and then propagate down stream with the cross flow. From previous experiments it has been seen that the inclusion of a ZNMF - jet can increase the mixing with the free stream fluid [3].

It has been shown that non-dimensional parameters such as Strouhal number, Reynolds and velocity ratio between the jet and free stream can be used to characterize the system. Previous experiments have shown that by changing the Strouhal number that the jet interacting with the free stream may experience two distinct flow regimes, a single trajectory flow seen at lower Strouhal numbers and a multiple trajectory flow at higher Strouhal numbers. It was also noticed that the higher Strouhal number flows resulted in with multiple trajectory regimes could penetrate further into the free stream. It should be noted that these flow regimes were seen in the mean flow, not instantaneous flows [1,4,11].

This investigation uses flow parameterisation from [1] to compare the physical properties of the flow structure in the mean

by changing the Strouhal number for a circular ZNMF - Jet in cross flow and holding the Reynolds number and Velocity Ratio constant.

### Nomenclature

$a$	=	piston amplitude
$D$	=	diameter of jet orifice plate
$d_p$	=	diameter of the piston
$f$	=	frequency of oscillation
$\rho_w$	=	density of water
$Re$	=	Reynolds number
$St$	=	Strouhal number
$U_\infty$	=	free stream velocity
$U_j$	=	momentum jet velocity
$\mu_w$	=	viscosity of water
ZNMF	=	zero-net-mass-flux
PIV	=	Particle Image Velocimetry
PLIF	=	Planar Laser Induced Fluorescence

### Experimental Technique

#### Particle Image Velocimetry

Particle image Velocimetry is a non-intrusive, optical velocity measurement technique in which the velocity field is measured indirectly by recording images of the light scattering tracer particles within the flow. A plane of interest in the flow is illuminated by 2 successive pulses of a coherent thin light sheet (for this experiment by a laser) spaced a short pre-determined time apart. The light scatter from the tracer particles is then captured through a single exposure photographic method for each of the two successive pulses on a CCD array. These two single-exposed images are then divided into regions known as interrogation windows (IW) and a cross-correlation algorithm is then performed on each exposure over local IW. Using the known time delay between the two exposure images and each particles displacement in successive IW their individual velocities are calculated. Further processing of the velocity data in two-dimensional directions may also be calculated to find more information, such as the vorticity of the flow field [9].

#### Flow Geometry

The ZNMF - JICF was generated in the Laboratory for Turbulence Research in Aerospace and Combustion at Monash University in the closed circuit vertical water tunnel, with a 1.5m long, 250mm square working section made of 15mm thick Perspex, shown in figure 1. The water is introduced through a spray system into a settling chamber at the top of the working section, which is then passed through a perforated plate, four stainless steel wire screens, a honeycomb and a 16:1 contraction before entering the working section [11]. This provides a smooth, uniform flow in the working section, with a free-stream turbulence intensity of less than 1% [7]. The ZNMF - Jet is created by a horizontally mounted scotch-yoke piston-cylinder arrangement, which has the ability to change through a number of discrete amplitudes. The piston diameter was  $d_p = 20\text{mm}$  while the jet orifice into the free stream was  $D = 10\text{mm}$ . This was

forced by a RM29B2S stepper motor controlled by a computer system, where the angular velocity of the motor was able to be set. Table 1 has a list of amplitudes with their maximum allowable frequencies of oscillation from the stepper motor [1].

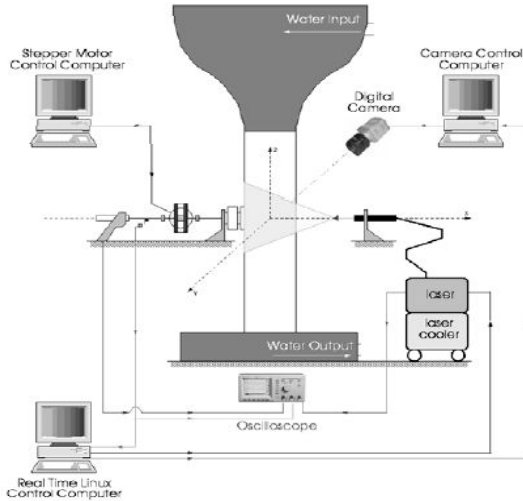


Figure 1. Schematic of experimental setup (Tomar, 2005).

<b>a</b>	1	2	4	6	10	14	22
<b>f</b>	5	6	8	8	6	4	2

Table 1. Maximum frequencies, f (Hz) of stepper motor as function of amplitude, a (mm).

### Image Acquisition

The acquisition apparatus used for the experiments was a PCO Pixelfly monochromatic camera, with full resolution of 1280 x 1024 pixels<sup>2</sup> per image, the results of this camera will be discussed in this paper. The experiments were also repeated using a PCO 4000 CCD array, with a higher full resolution of 4008 x 2672 pixels<sup>2</sup> per image, the results and discussion of which are reported in [2].

The Calibration of spatial resolution was determined by calibrating the front and rear faces of the tunnel working section. These resolutions were linearly interpolated to find the resolution where the laser sheet was illuminated. These spatial resolution calibrations were checked before and after each experiment to ensure they remained accurate. This was necessary because the working section of the vertical water tunnel used is not accessible without draining the water and removing the perspex plates on the exterior of the tunnel.

### Phase Locking

Phase locking refers to sampling images at a single point in the oscillation of a forcing mechanism, this means information about a specific time in the period of the mechanism can be identified as opposed to only time averaged information seen by randomly taking images in the oscillation. Phase locking may be used in an experiment if the forcing mechanism of the fluid has an oscillating motion associated with it. The use of a ZNMF – Jet allows the PIV experiments to be phase locked. This was achieved by setting the acquisition and laser timing frequency to be either equal to or a multiple of the forcing frequency. The period of oscillation was split into 16 equally spaced phases, 22.5° apart with the origin, 0° phase being at the maximum velocity of the piston in the exhaust point of the cycle, See figure

2. Using the PCO Pixelfly camera 400 samples were taken at each phase, while for the PCO 4000 array 60 samples were taken.

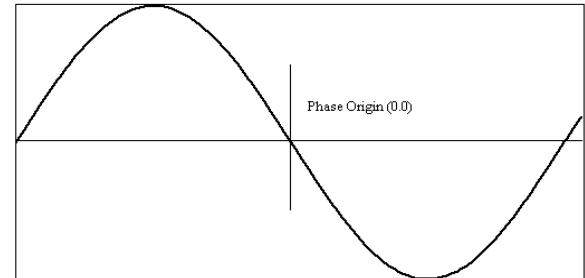


Figure 2. Phase locking origin description.

### Experimental Parameters

A ZNMF – Jet in cross-flow has a number of non-dimensional parameters associated with its flow characteristics. These are the Reynolds number (Re) and the Strouhal number (St). A final non-dimensional parameter of velocity will also be used to relate the ZNMF – Jet and free stream.

$$Re = \frac{\rho_w U_j D}{\mu_w} \quad (1)$$

$$St = \frac{fD}{U_j} \quad (2)$$

$$VR = \frac{U_j}{U_\infty} \quad (3)$$

It can be shown that these non-dimensional parameters can be expressed in terms of only the geometric parameters of the ZNMF – Jet and free stream and forcing parameters of the ZNMF – Jet [11] See Equations (4-6).

$$St = \frac{D^2}{\sqrt{2\pi} d_p a} \quad (4)$$

$$Re = \frac{\sqrt{2\pi} f a d_p}{v_w} \quad (5)$$

$$VR = \frac{U_j}{U_\infty} \quad (6)$$

It can therefore be seen that the  $St$  is only a function of the amplitude of the piston motion, while  $Re$  is a function of both frequency and amplitude. With the other parameters being constant for the system.

**Experimental Conditions**

By maintaining a constant multiple of frequency of oscillation and amplitude the  $St$  number can be changed while keeping a constant  $Re$ . This can be done without changing the  $VR$ . Table 2 shows the experimental conditions used.

	Experiment 1	Experiment 2
$f$ (Hz)	1.2	6
$a$ (mm)	10	2
$U$ (mm/s)	53	53
$U_i$ (mm/s)	106	106
$St$	0.11	0.56
$Re$	1066	1066
$VR$	2	2

Table 2. Experimental conditions for PIV experiments.

**Results and Discussion**

**Mean Flow Structures**

The following figures show time averaged velocity magnitude contours and are compared against PLIF results from [4].

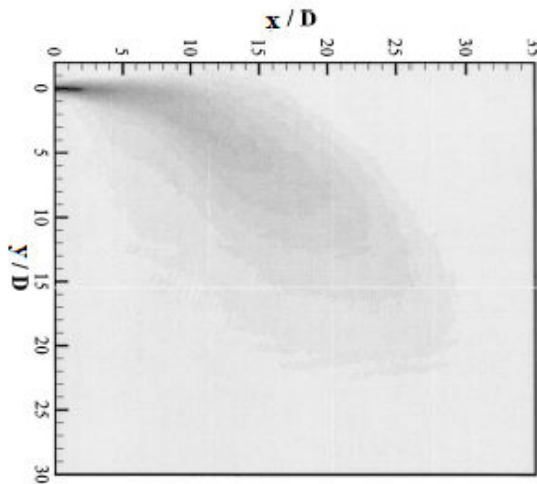


Figure 3. PLIF experiment from [4], singular trajectory.

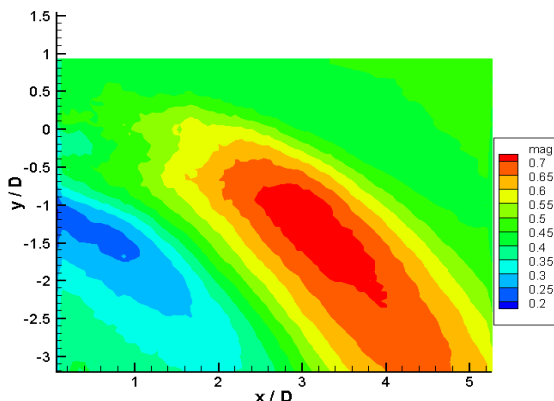


Figure 4. Mean velocity magnitude /  $U_\infty$ ,  $St = 0.11$ ,  $f = 1.2\text{Hz}$ ,  $a = 10\text{mm}$ .

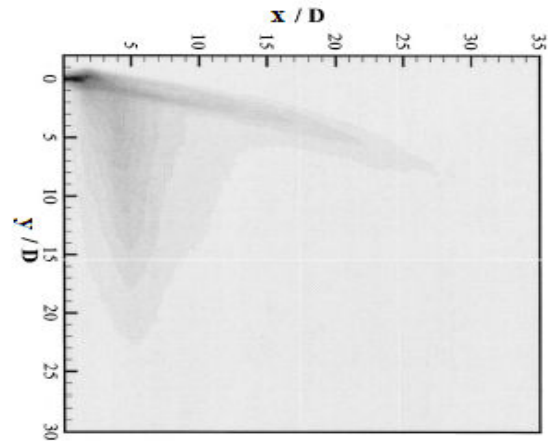


Figure 5. PLIF experiment from [4], multiple trajectory.

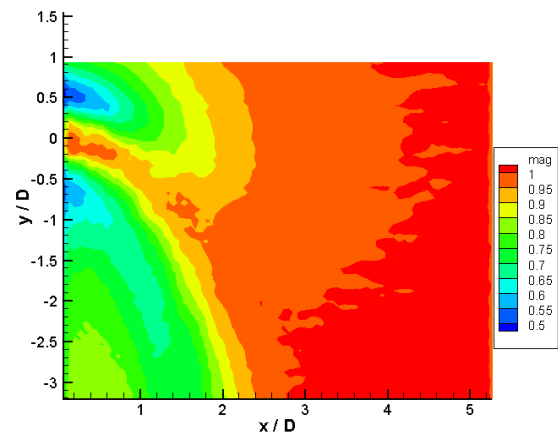


Figure 6. Mean velocity magnitude /  $U_\infty$ ,  $St = 0.56$ ,  $f = 6\text{Hz}$ ,  $a = 2\text{mm}$ .

The PLIF results in figures 3 and 5 are from past experiments and are being used here only as a comparison. What can be seen is that for  $St = 0.11$  the PIV velocity magnitude, figure 4 the flow showed a single trajectory flow of high velocity, similar to what was seen in the PLIF experiments in figure 3 which is in the regime of low Strouhal number where the flow is expected to show a single trajectory. The higher Strouhal number of 0.56 again correlated well with what was seen in the previous PLIF experiments where a multiple jet trajectory was seen, figure 5 in the PIV plot, figure 6 a high velocity jet was found penetrating almost horizontally into the free stream, below this a small region of low velocity can be seen and then a again a region of higher velocity beneath that.

In comparing between the two Strouhal number velocity results it is interesting in these comparison plots that the lower Strouhal number experiment, figure 4 appears to show a further penetration into the free stream before the trajectory of higher velocity flow is diffused into the free stream, occurring at approximately  $x / D = 5$  into the free stream. But in the higher Strouhal number results this occurred at about  $x / D = 2$ . In previous experiments it was the higher Strouhal number experiments that showed a longer penetration into the bulk fluid. In relation to comparing the PLIF experiments to PIV results it should be noted from [5] that in flows that exhibit turbulent properties such as ZNMF – JICF interpretation of PLIF results

that follow streak lines in the flow should be done with great care as previous comparisons of this nature have found differences in the technique results [8].

**Vortical Structures**

Figures 7 and 8 show results from the phase locked experiments at a phase of 22.5°, similar plots have been created at each of the phases, and these show the beginning of a jet being forced into the free stream. Both St number results show two vortices on the boundary of the jet forcing into the free stream, one on the upper surface rotating counter clockwise and the other rotating clockwise on the lower side of the jet. They also show the remnant vortical streams from the preceding jet. This stream shows a similar penetration into the free stream as in figure 4 and 6. What should be noted here is that there is a difference between the strength of the vortex on the lower and upper surface of the jet stream. In both cases the lower vortex shows significantly higher strength, approximately 2:1 in both cases between the lower and upper vortex. This is of note because in the later phases of the cycle the ratio of vortex strength between the upper and lower structure is approximately 1, which means that the lower vortex is being diffused into the free stream at a quicker rate at the beginning of the period of oscillation than the upper. What is also seen is that for St = 0.11 the vortical strength is higher on both the upper and lower structures and this may be a reason for the further penetration of this case into the free stream.

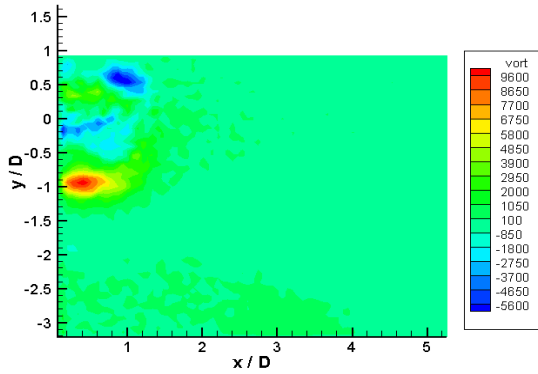


Figure 7. Vorticity, St = 0.11, f = 1.2Hz, a = 10mm.

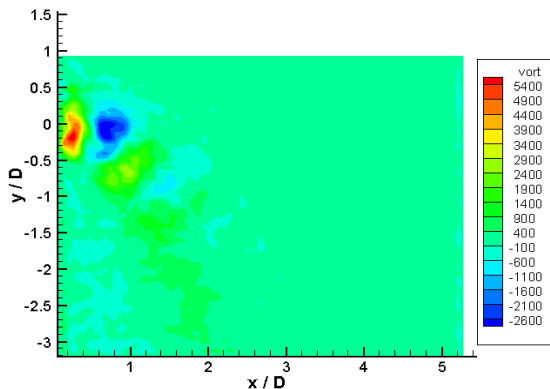


Figure 8. Vorticity, St = 0.56, f = 6Hz, a = 2mm.

**Phase Averaged Velocity**

“Velocity signals in the wake-transition regime are periodic but include three-dimensional perturbations originated from the existence of the secondary vortices.” – [10]. This is shown in equation (7).

$$u(\vec{x}, t) = \bar{u}(\vec{x}) + \tilde{u}(\vec{x}, t) + u'(\vec{x}, t) \tag{7}$$

where:

$$\bar{u}(\vec{x}) = \lim_{T \rightarrow \infty} \frac{1}{T} \int_0^T u(\vec{x}, t) dt \tag{8}$$

$$\langle u(\vec{x}, t) \rangle = \lim_{N \rightarrow \infty} \frac{1}{N} \sum_{n=0}^{N-1} u(\vec{x}, t + n\tau) \tag{9}$$

Where  $\bar{u}(\vec{x})$  is the global mean component of the velocity,  $\tilde{u}(\vec{x}, t)$  is the periodic mean component and  $u'(\vec{x}, t)$  is a random component according to the triple decomposition [6]. The Periodic mean components are shown in figures 9 and 10 at one phase for each condition to show the relative maximum penetration in to the free stream. On each of the plots the jet origin is at (0,0)

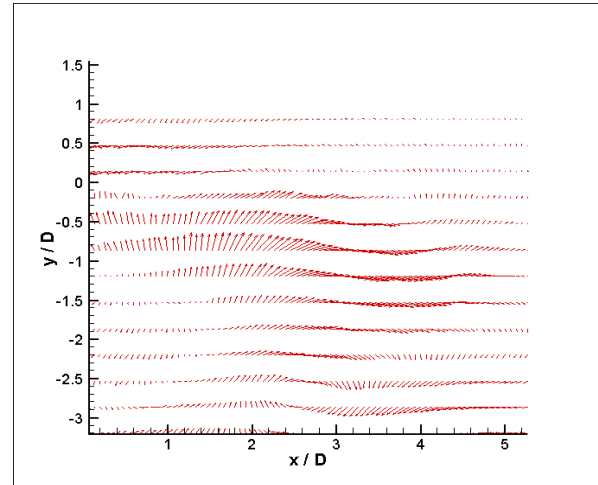


Figure 9. Velocity vectors, Phase = 157.5° St = 0.11, f = 1.2Hz, a = 10mm.

It can be confirmed again from figures 9 and 10 that the lower St experiment resulted in the ZNMF – Jet penetrating further into the free stream. With Fig. 10 showing the evolution of the jet period the velocity of the free stream is perturbed by a large amount up to x / D = 5 while the higher St experiment did not disrupt the flow more than about x / D = 2.

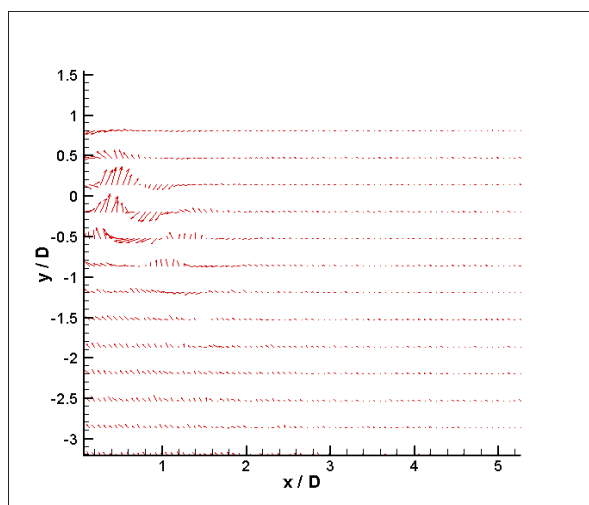


Figure 10. Velocity vectors, Phase =  $157.5^\circ$   $St = 0.56$ ,  $f = 6\text{Hz}$ ,  $a = 2\text{mm}$ .

### Conclusion

A quantitative research project has been completed on ZNMF – JICF. It has been seen in the mean velocity field that for low  $St$  a singular trajectory jet was seen penetrating into the free stream, while for a higher  $St$  a multiple trajectory flow was seen for the jet penetrating into the free stream, which is consistent with previous results. However it was seen that the lower  $St$  penetrated further into the stream in both the mean and phase averaged results while in previously conducted PLIF experiments it was concluded that the higher  $St$  cases penetrated further into the bulk free stream. The vorticity of the cases showed bias of strength to the lower vortical structures when exiting the jet orifice. The lower  $St$  case showed higher vortical strength and may be a reason for the increased penetration of the singular trajectory jet into the free stream.

### References

- [1] Arnaud, J., Tomar, S., and Soria J., *Investigation of the Mean Flow Pattern in Zero-Net-Mass-Flux Elliptical-Jets in Cross-Flow using Planar-Laser-Induced Fluorescence*, 15<sup>th</sup> Australian Fluid Mechanics Conference, Sydney, Australia, 2004, pp. 13-17.
- [2] Dillon-Gibbons, C., *Mean field structures of a zero-net-mass-flux jet in cross flow*, Honours Thesis, Laboratory for Turbulence Research in Aerospace Combustion, Mechanical Engineering Dept, Monash University, Melbourne, Australia, 2006.
- [3] Eroglu, A., and Breidenthal, R. E., *Effects of Periodic Disturbances on Structure and Flame Length of a Jet in a Cross Flow*, AIAA Paper 91-0317, Aerospace Sciences Meeting, 29<sup>th</sup>, Reno, NV, Jan. 7-10, 1991.
- [4] Gordan, M., Cater, J. E., Soria, J., *Investigation of the mean passive scalar field in zero-net-mass-flux jets in cross-flow using planar-laser-induced fluorescence*, Physics of Fluids, Vol. 16 Num. 3, March 2004, pp. 794-808.
- [5] Hama, F. R., *Streaklines in a perturbed shear flow*, Phys Fluids, 1962, Vol. 5, pp. 644-650.
- [6] Hussain, A.K., Reynolds, W.C., *The mechanics of an organized wave in turbulent shear flow*. Journal of Fluid Mechanics Vol 41, pp. 241-258. 1970.
- [7] Nicolaides, D., *Measurement of spatial quantities in grid turbulence using particle image Velocimetry*. Master's thesis, Monash University, Melbourne, Australia, 1997.
- [8] O'Neill, P., Soria, J., Honnery, D., *The stability of low Reynolds number round jets*, Experiments in Fluids, 2004, Vol. 56, pp. 473-483.
- [9] Soria, J., Masri, A., Honnery, D., *An adaptive Cross Correlation Digital PIV Technique for Unsteady Flow Investigations*, Proc. 1<sup>st</sup> Australian conference on Laser Diagnostics in Fluid Mechanics and Combustion, Sydney, Australia, 1996, pp. 29-45.
- [10] Sung, J., Yoo, J.Y., *Three-dimensional phase-averaging of time-resolved PIV measurement data*. Measurement Science and Technology 12, pp. 655-662 2001.
- [11] Tomar, S., Arnaud, J., and Soria, J., *Zero-Net-Mass-Flux Jets in Cross-Flow*, 8th Australian Heat and Mass Transfer Conference, Perth, Australia, 2005, pp. 26-29.